Chinese Journal of Chemical Engineering 53 (2023) 402–408

Contents lists available at ScienceDirect

Chinese Journal of Chemical Engineering

journal homepage: www.elsevier.com/locate/CJChE

Full Length Article

Influence of Ca/P ratio on the catalytic performance of hydroxyapatite for decarboxylation of itaconic acid to methacrylic acid

Shutong Pang, Hualiang An *, Xinqiang Zhao *, Yanji Wang

Hebei Provincial Key Laboratory of Green Chemical Technology and Efficient Energy Saving, Tianjin Key Laboratory of Chemical Process Safety, School of Chemical Engineering and Technology, Hebei University of Technology, Tianjin 300130, China

ARTICLE INFO

Article history:
Received 10 September 2021
Received in revised form 10 January 2022
Accepted 12 January 2022
Available online 25 January 2022

Keywords:
Biomass-derived itaconic acid
Methacrylic acid
Hydroxyapatite catalyst
Ca/P ratio
Decarboxylation reaction

ABSTRACT

Methacrylic acid, an important organic chemical, is commercially manufactured starting from fossil feedstock. The decarboxylation of itaconic acid derived for biomass is a green route to the synthesis of methacrylic acid. In view of the problems existing in the researches on this route such as use of noble metal catalyst, harsh reaction conditions and low desired-product yield, we prepared a series of hydroxyapatite catalysts with different Ca/P molar ratios and evaluated their catalytic performance. The results showed that the hydroxyapatite catalyst with a Ca/P molar ratio of 1.58 had the best catalytic activity. The highest yield of MAA up to 61.2% was achieved with basically complete conversion of itaconic acid under the suitable reaction conditions of 1 equivalent of NaOH, 2 MPa of N_2, 250 °C, and 2 h. On this basis, a reaction network for the decarboxylation of itaconic acid to methacrylic acid catalyzed by hydroxyapatite was established. With the aid of catalyst characterization using X-ray powder diffraction, NH_3/CO_2 temperature-programmed desorption, N_2 physisorption, inductively coupled plasma optical emission spectrometry, and scanning electron microscopy, we found that the distribution of surface acid sites and basic sites, crystal growth orientation, texture properties and morphology of hydroxyapatite varied with the Ca/P molar ratio. Furthermore, the change of the crystal growth orientation and its influence on the surface acidity and alkalinity were clarified.

1. Introduction

Methacrylic acid (MAA) is an important monomer widely used in the production of methacrylates (*e.g.*, methyl methacrylate), organic glass, polymers, paints, adhesives and coatings, *etc* [1]. Global production of methyl methacrylate is expected to reach 6 million tons in 2023 [2], greatly stimulating the manufacture and technological development of MAA. Currently, methyl methacrylate is mainly produced from fossil resources such as acetone cyanohydrin process or through the oxidation of isobutene, and the acetone cyanohydrin process accounts for 60.6% [3,4]. This unsustainable method depends on the use of expensive and extremely toxic feedstocks alongside corrosive concentrated acids. Besides the use of harmful substrates, low atom economy, poor product selectivity and the net emission of greenhouse gases are also the drawbacks associated with the industrial process, not to mention that the production is exclusively based on non-renewable resource [5]. In addition to isobutylene oxidation and acetone cyanohydrin methods, C_2 routes (*e.g.*, BASF process starting from ethylene), C_3 routes (process based on propane, propylene, and proyne), and C_4 routes (process based on isobutene/t-butanol, isobutane partial oxidation, *etc.*) have also been developed [6]. However, all of them are based on non-renewable fossil feedstocks. With the increasing awareness of environmental protection and intensive research on the chemical utilization of biomass, chemical industry is shifting to utilizing green synthetic process based on biomass feedstocks [7]. The synthesis of MAA by biomass platform molecules has attracted great interest [8–10], especially starting from itaconic acid [11,12]. Itaconic acid is an important bio-derived platform compound [13,14] and can be a potential substitute for petroleum-derived chemicals such as acetone cyanohydrin, maleic acid or acrylic acid [15,16]. Currently, no commercial routes to the synthesis of bio-based MAA or methyl methacrylate are available, but several companies and academic research groups have reported their results. Lucite corporation applied several patents related to the preparation of MAA by itaconic acid [17–19]. Carlsson's group [20] obtained up to 72% of MAA yield using caustic soda catalyst under near-critical and supercritical water conditions (250–400 °C and 20–34.5 MPa),

* Corresponding authors.
E-mail addresses: anhl@hebut.edu.cn (H. An), zhaoxq@hebut.edu.cn (X. Zhao).

https://doi.org/10.1016/j.cjche.2022.01.012
1004-9541/

but the harsh reaction conditions limit the development of this process. Notre's group [21] utilized Pt/Al_2O_3 and caustic soda catalyst for decarboxylation of itaconic acid and achieved a MAA yield of 68%. However, the use of noble metal Pt increases the process cost. In order to avoid the use of expensive noble metals, Pirmoradi *et al.* [22] employed hydrotalcite as a solid catalyst for MAA synthesis, confirming the feasibility of solid acid-base catalysts for the decarboxylation of itaconic acid in spite of relatively lower MAA yield (23%). In general, homogeneous catalysts have superior selectivity and specificity compared with their heterogeneous counterpart. Lansing *et al.* [23] obtained 95.2% MAA selectivity with only 42% conversion of itaconic acid using ruthenium carbonyl complex catalyst $[Ru(CO)_2(CH_3CH_2COO)]_n$ at 225 °C and 2.8 MPa. Furthermore, homogeneous catalysis also means additional difficulty in separation of the reaction products, increasing production costs and operational complexity. Bohre *et al.* [24] applied barium hexaaluminate to catalyze the decarboxylation of itaconic acid and obtained 50% yield of MAA. In summary, metal, acid and base sites have catalytic effects on the decarboxylation of itaconic acid, and the role of acid-base sites is particularly important.

Hydroxyapatite is widely used in catalysis due to its strong adsorption, surface acid-base tunability and strong ion-exchange properties [25]. By changing Ca/P molar ratio to adjust the acidity and alkalinity, hydroxyapatite has been successfully applied to the catalytic conversion of biomass feedstocks such as ethanol Guerbet reaction [26] and lactic acid dehydration reaction [27,28]. However, to the best of our knowledge, there are no reports concerning the catalytic application in the decarboxylation of itaconic acid to MAA. In this work, we prepared a series of hydroxyapatite catalysts with different Ca/P molar ratios by controlling the pH of the mixed solution in hydrothermal synthesis. The morphology, textural structure and acid-base properties of the as-prepared hydroxyapatite catalysts were characterized. The catalytic activity evaluation results showed that a MAA yield of 61.2% was achieved with basically complete conversion of itaconic acid without the use of noble metals and under mild conditions.

2. Materials and Methods

2.1. Catalyst preparation

Four hydroxyapatite catalysts were prepared by the hydrothermal method [26,29]. Typically, 16.68 g of $Ca(NO_3)_2{\cdot}4H_2O$ and 5.84 g of $(NH_3)_2HPO_4$ were separately dissolved in 176 ml and 146 ml of deionized water. Then the aqueous solution of $(NH_3)_2HPO_4$ was fed slowly into the aqueous solution of $Ca(NO_3)_2{\cdot}4H_2O$ under gentle agitation. The mixture remained stirring for 3 h and aging for 3 h. The pH of the mixed solution varied from 7 to 10 by adjusting the addition amount of a 28% (mass) aqueous ammonium hydroxide solution. The whole process was conducted in a water-bath controlled at 40 °C. The mixture was then transferred to an autoclave for a hydrothermal process for 12 h at 130 °C. A white precipitate was separated by centrifugalization at 10000 $r{\cdot}min^{-1}$ and washed sequentially with ethanol for 5 min (quartic). Finally, the hydroxyapatite catalysts with different Ca/P molar ratio were obtained after dried at 90 °C for 24 h. The different samples prepared at a pH of 7, 8, 9 and 10 were separately marked as HAP-1, HAP-2, HAP-3 and HAP-4.

2.2. Catalyst characterization

The crystalline phases of the catalyst samples were confirmed by powder X-ray diffraction (XRD) analysis on a Bruker D8 Discover X-ray diffractometer with Cu K_α (λ = 0.15418) radiation at 100 mA and 40 kV. The patterns were recorded for 2θ angles between 10° and 90° at a rate of 6 (°) $\cdot min^{-1}$. Bulk Ca/P molar ratio of the catalyst samples were determined by inductively coupled plasma optical emission spectrometry (ICP-OES) using an Opfima 7300 V device. The specific surface area and pore size distribution of the catalysts were measured on the ASAP2020M C specific surface and porosity analyzer. The NH_3-TPD and CO_2-TPD tests were carried out in a self-assembled glass U-shape reactor system coupled with a thermal conductivity detector (TCD). The morphological appearance of the catalyst samples was observed by scanning electron microscopy (SEM) using a Nova Nano SEM450 scanning electron microscope.

2.3. Catalytic performance evaluation

The catalytic performances of the catalysts for the decarboxylation of itaconic acid were evaluated in a 100 ml autoclave. In a typical experiment, 0.4 g of itaconic acid and 0.12 g NaOH were dissolved in 20 ml of deionized water. The solution was transferred into the autoclave charged with 0.8 g of catalyst. After sealed, the autoclave was purged three times with N_2 before heated to the desired temperature. Once the reaction was completed, the autoclave was cooled down to room temperature and the residual gas was released. The reaction solution was recovered by a microfiltration operation and the filtrate was diluted with deionized water prior to analysis by a high performance liquid chromatography (HPLC). The analysis of the liquid samples was performed by using a Waters 1525 HPLC equipped with an Acclaim™ Organic Acid LC Columns (5.0 μm; 4 × 25 mm) heated to 45 °C and with a Waters 2998 PDA detector. The mobile phase consisted of an aqueous phase (4 $mmol{\cdot}L^{-1}$ H_2SO_4 solution) and organic phase (acetonitrile) and its flow rate was controlled at 1.0 $ml{\cdot}min^{-1}$. A gradient method [24] was employed as follows, started with 100% of the aqueous phase, changed to 90% of organic phase in 5 min and kept it for 3 min. Then the gradient program was reversed to go back to 100% of aqueous phase in 5 min. The components were quantified by an external standard method.

3. Results and Discussion

3.1. Characterization of hydroxyapatite catalysts

Fig. 1 shows XRD patterns of the four hydroxyapatite catalysts. The diffraction peaks are in good agreement with JCPDS 74-0566.

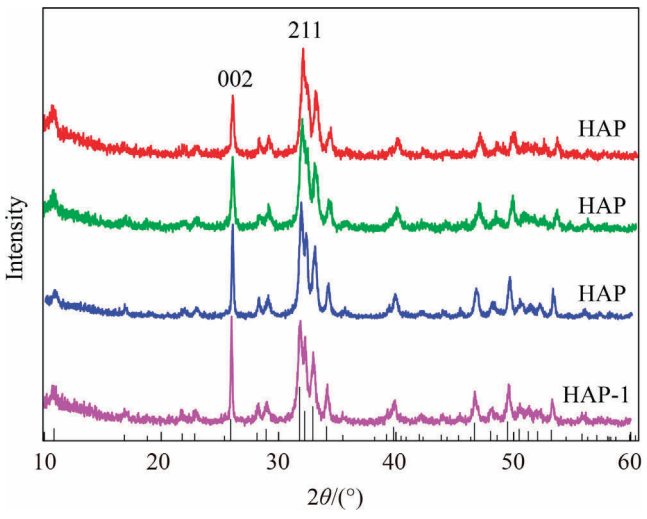

Fig. 1. XRD patterns of the four hydroxyapatite catalyst powders.

The strong and sharp diffraction peaks indicate that a relatively pure hydroxyapatite crystalline phase was obtained in the hydrothermal process at 130 °C. However, a distinct variation of peak intensity in the facet of (0 0 2) can be clearly observed, indicating that different hydroxyapatite samples may have different preferred orientation. With a gradual increase of pH in the preparation process, the relative intensity of the diffraction peak at 2θ = 25.9° and that at 2θ = 31.8° gradually became weaker. The most intense diffraction peak of HAP-1 was at 2θ = 25.9° while that of HAP-4 was at 2θ = 32.8°. The preferred orientation can be deduced from the ratio of diffraction peak intensity. Dokko *et al* [30] found that if the ratio of $I_{(020)}/I_{(200)}$ (ratio of diffraction peak intensity in {0 2 0} plane to that of {2 0 0} plane) was greater than that of the standard, the prominent {0 2 0} plane would be observed. They suggested that the crystal orientation changed depending on the concentration and pH of the precursor solution. Wang *et al* [31] also drew the inference of a crystal preferred orientation by comparing the measured $I_{(020)}/I_{(200)}$ with the standard value. In this work, the $I_{(002)}/I_{(211)}$ ratio of JCPDS-74-0566 is 0.36 while the ratio of HAP-1, HAP-2, HAP-3, and HAP-4 are separately 1.12, 0.84, 0.68, and 0.61. Therefore, we suggest that the crystal orientation of the hydroxyapatite sample likewise varied with the change of the pH of the precursor solution. The preferred orientation of the hydroxyapatite crystals prepared at a low pH is {0 0 2} plane. As the pH increases, the preferred orientation gradually shifts to {2 1 1} plane. We believe that this difference arises from the process of hydroxyapatite synthesis because tabular brushite ($CaHPO_4{\cdot}2H_2O$) is precipitated as a precursor in the precipitation solutions with a low pH and gradually transformed into hydroxyapatite [32,33].

Fig. 2 shows the SEM images of the four hydroxyapatite catalysts. Different degrees of agglomeration can be observed in all samples. It is found from the above XRD analysis that the preferred orientation of HAP-1 is {0 0 2} crystal plane. The SEM image showed that HAP-1 appears platelike. The preferred orientation of HAP gradually starts to change to the {2 1 1} crystal plane with an increase in the pH of the precursor solution. HAP-2 is still platelike, but the ratio of length to diameter is larger than that of HAP-1. When the pH of the precursor solution was 9, HAP-3 changed into a rodlike particle. When the pH of hydroxyapatite crystalline growth environment is 10, HAP-4 is also rodlike but its length gets shorter. With an increase of Ca/P molar ratio, the particle size of hydroxyapatite becomes smaller, causing the increase of its specific surface area. This result is similar to the results of Tsuchida *et al* [26]. They found that hydroxyapatite appeared platelike when the Ca/P molar ratio was low and that it had smaller particles and consequently higher specific surface area with a high Ca/P molar ratio.

The results of ICP analysis (Table 1) show that the bulk Ca/P molar ratios of hydroxyapatite gradually increased as the pH of the precursor solution was elevated. The change in the Ca/P molar

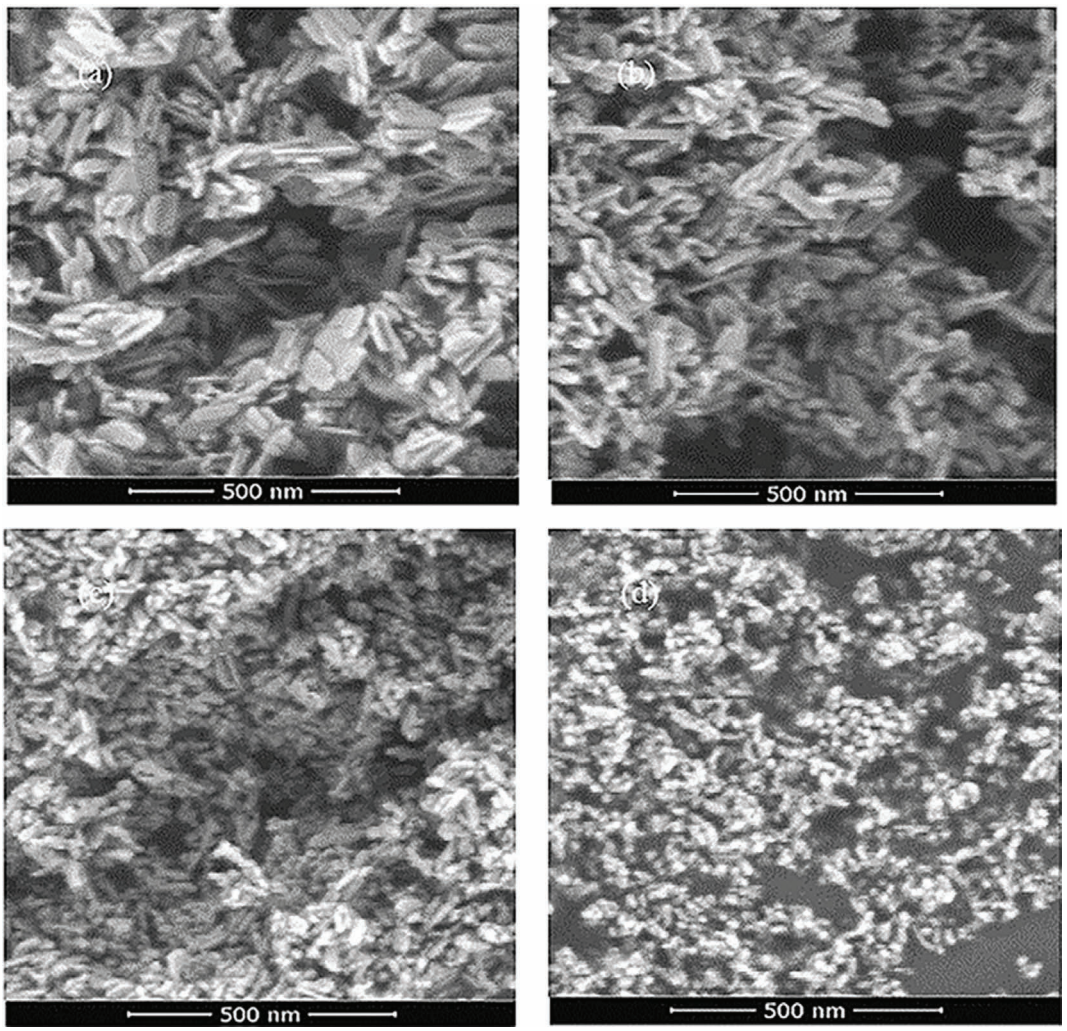

Fig. 2. SEM images of (a) HAP-1, (b) HAP-2, (c) HAP-3, and (d) HAP-4.

ratio of hydroxyapatite with the pH of the precipitation solution derives from the form of the phosphate anion (*i.e.*, $H_2PO_4^-$, HPO_4^{2-}, and PO_4^{3-}) presented in the solution. As the pH of the solution rises, PO_4^{3-} is the main form of phosphate anion present in the solution [34], favouring the formation of hydroxyapatite sample with high Ca/P molar ratio [26]. The textural properties of the hydroxyapatite samples were analyzed and the results are also listed in Table 1 and the adsorption isotherms are shown in Fig. S1 in the Supplementary Material. The specific surface area and pore volume of all the samples increased with the pH of the precipitation solution. According to the IUPAC classification, the physisorption curves of four hydroxyapatite samples belong to type IV with a H_2 hysteresis loop, indicating that they all possess mesoporous structures (pore size 2–50 nm), and the pore size distribution is relatively uniform.

Table 2 gives the strength and density of the acid sites and basic sites on the surface of hydroxyapatite catalysts while the profiles of CO_2-TPD and NH_3-TPD are showed in Fig. S2 in Supplementary Material. The desorption temperatures of CO_2 and NH_3 gradually rose with the increase of Ca/P molar ratio, indicating that the strength of acidity and alkalinity increased with the increase of Ca/P molar ratio [28]. However, none of them contained strong acid sites and strong alkaline sites. It is known that the acid/basic property of nonstoichiometric hydroxyapatite is governed by its Ca^{2+} ions, that is, its basic property derives from the presence of Ca^{2+} ions and its acidic property derives from the deficiency of Ca^{2+} ions [32,33]. Therefore, with the increase of Ca/P molar ratio, the density of acidic sites on the surface of hydroxyapatite gradually decreased and that of basic sites gradually increased. In addition, Tsuchida *et al* [26] suggested that the surface acidity and basicity of hydroxyapatite is related to its crystal growth. For the crystals with a low Ca/P molar ratio, more phosphate groups associated with acidity was exposed. For the crystals with a high Ca/P molar ratio, more calcium-bearing faces was exposed, resulting in high basic site density. Our observations confirm that there are differences in the preferential orientation of hydroxyapatite crystal growth at different Ca/P molar ratios, and the highest amount of acid sites was found in HAP-1 while the highest amounts of base sites was found in HAP-4.

3.2. Catalytic performance for decarboxylation of itaconic acid

The catalytic performance of the hydroxyapatite catalysts was tested for the decarboxylation of itaconic acid and the results are given in Table 3. Under the studied reaction conditions, the conversion of itaconic acid was essentially complete but the MAA yields varied over the hydroxyapatite catalysts with different Ca/P molar ratios, indicating that the Ca/P molar ratio significantly affected the catalytic selectivity. Previous reports noted that effective catalysis for the decarboxylation of itaconic acid depends on the basicity of the catalyst [20,35]. The catalyst with moderate basicity facilitates the decarboxylation reaction of itaconic acid. For instance, HAP-1 and HAP-4 catalysts separately with low and high basicity afford a MAA yield of 43% and 35% under the studied reaction conditions. In contrast, HAP-2 and HAP-3 catalysts exhibited moderate basicity and respectively gave a relatively high MAA yield of 55% and 61%. The experimental results indicate that the acid-base properties of hydroxyapatite with a Ca/P molar ratio of 1.58 is more suitable for the synthesis of MAA by decarboxylation of itaconic acid.

Since HAP-3 showed the best catalytic performance, the effect of reaction conditions was tested and the results are shown in Table 4. At low temperatures (190–220 °C), itaconic acid conversion is incomplete and the yield of MAA is low. Increasing the temperature to 220 °C resulted in a significant improvement in both itaconic acid conversion and MAA yield despite a high percentage of itaconic acid isomers existed (21%). The highest yield of MAA was achieved at a temperature of 250 °C. Continuing to increase the temperature to 260 °C caused a decrease in MAA yield, probably because high temperature led to more side-reactions (decarboxylation and hydration) of MAA [20] and a poor product selectivity.

Basicity plays an important role in the decarboxylation of itaconic acid. The use of moderate amounts of bases promotes the dissociation of itaconic acid to form a monoanion form, which is more readily decarboxylated to MAA as compared to neutral and dianion forms [36,37]. The HAP-3 showed a good catalytic activity with a MAA yield of 47% in absence of NaOH. As the amount of NaOH was increased to the molar ratio of NaOH to itaconic acid = 0.5:1, the reaction results did not show significant change. The highest yield of MAA was achieved when the molar ratio of NaOH to itaconic acid reached 1:1. However, the yield of MAA showed a serious decline with a continuous increase in the amount of NaOH. Li and Brill [37] reported that the reaction rate of itaconic acid decarboxylation is dependent on the pH of the reaction mixture and too high a pH quenches the decarboxylation reaction [20]. Using NaOH alone as a catalyst at 250 °C, the MAA selectivity was poor (only 10%) although the conversion of itaconic acid was high [20,24]. This situation was improved significantly with the addition of hydroxyapatite. The high catalytic activity of hydroxyapatite may be due to its stabilizing effect on the monoanion form of itaconic acid by providing a suitable basic site [37]. As mentioned above, MAA is more readily converted from the monoanion form of itaconic acid. Lansing suggested [23] that suitable Lewis acid sites

Table 1
Ca/P molar ratio and textural properties of the hydroxyapatite samples

Catalyst	pH	Ca/P molar ratio	BET/$m^2 \cdot g^{-1}$	Pore volume/$m^2 \cdot g^{-1}$
HAP-1	7.0	1.46	76.28	0.23
HAP-2	8.0	1.51	81.42	0.24
HAP-3	9.0	1.58	85.63	0.34
HAP-4	10.0	1.69	90.94	0.36

Table 2
Acid and base properties of different hydroxyapatite samples

Catalyst	Acidity/$\mu mol \cdot g^{-1}$			Basicity/$\mu mol \cdot g^{-1}$		
	Weak (<200 °C)	Medium (200–400 °C)	Total acid amount	Weak (<200 °C)	Medium (200–400 °C)	Total base amount
HAP-1	138.35	198.62	336.98	55.31	89.65	144.96
HAP-2	112.89	193.38	307.32	92.58	119.82	212.40
HAP-3	110.73	181.74	292.47	106.27	130.20	236.47
HAP-4	66.98	174.15	241.50	123.33	142.93	266.26

Table 3
Influence of Ca/P molar ratio of HAP on itaconic acid decarboxylation

Entry	Catalyst	Ca/P molar ratio	Conversion/%	Yield/%				
				MA	CA	CIA	MAA	Others
1	HAP-1	1.46	99.0	1.0	1.0	1.1	42.9	54.0
2	HAP-2	1.51	98.9	1.8	1.9	<1	54.7	40.6
3	HAP-3	1.58	98.7	2.3	1.1	<1	61.2	34.4
4	HAP-4	1.69	99.0	<1	<1	<1	34.6	62.4

Note: Reaction conditions are solvent (water, 20 ml), T = 250 °C, P = 2 MPa, time = 2 h, 1 equivalent of NaOH.
MA: mesaconic acid; CA: citraconic acid; CIA: crotonic acid.
Others: 2-hydroxyisobutyric acid, crotonic acid, propene and carbon dioxide.

Table 4
Influence of reaction conditions on itaconic acid decarboxylation over hydroxyapatite catalyst

Entry	T/°C	P/MPa	NaOH[①]/equiv.	Conversion/%	Yield/%				
					MA	CA	CIA	MAA	Others
1	190.0	2.0	1.0	91.4	39.9	1.3	1.2	21.3	36.3
2	220.0	2.0	1.0	97.6	17.5	2.8	1.0	52.8	25.9
3	250.0	2.0	1.0	98.7	2.3	1.1	<1	61.2	34.4
4	260.0	2.0	1.0	100.0	/	1.3	1.0	50.3	47.4
5	250.0	2.0	0.0	98.7	4.1	2.7	1.1	46.9	45.2
6	250.0	2.0	0.5	>99.9	<1	3	0.8	47.8	47.4
7	250.0	2.0	1.5	98.4	/	1.1	0.7	54.7	43.5
8	250.0	2.0	2.0	92.3	3	1.8	/	24.2	71.0
9	250.0	3.0	1.0	>99.9	1.8	3.2	1.7	58.2	35.1
10[②]	250.0	2.0	1.0	>99.9	/	/	/	56.8	43.2
11[③]	250.0	2.0	1.0	95.2	5.2	7.4	3.1	51.1	33.2
12[④]	250.0	2.0	1.0	>99.9	1.2	/	/	57.5	41.3

MA: mesaconic acid, CA: citraconic acid; CIA: crotonic acid.
Others: 2-hydroxyisobutyric acid, crotonic acid, propene and carbon dioxide.
① Molar ratio of NaOH to itaconic acid.
② Catalyst = 1.6 g.
③ Time,1 h.
④ Time,3 h.

also contribute to the decarboxylation of itaconic acid to MAA. The Lewis acid sites on the hydroxyapatite surface with a Ca/P ratio of 1.58 similarly promoted the reaction.

In line with our expectations, shortening reaction time to 1 h caused a decrease in MAA yield and an increase in by-products. If reaction time was extended to 3 h, the yield of MAA did not change significantly. Since almost no itaconic acid and its isomers were left in the reaction system after 2 h, the system pressure at 3 h did not change significantly compared with that at 2 h. This indicates that the components and their contents in the system do not change significantly after 2 h. In addition, the change of reaction pressure and catalyst dosages did not improve the MAA yield. It was found that the pressure at the end of the reaction was 0.1 to 0.2 MPa higher than the initial pressure at the required reaction temperature. The gas phase products were analyzed and mainly propylene and CO_2 were found, indicating the presence of degradation reaction in the system. This is consistent with the report by Carlsson *et al* [20]. They found that decarboxylation of itaconic acid to MAA was accompanied by excessive decarboxylation to produce propylene (up to 8%). According to the study by Li *et al.* [37], the formation of by-products can be explained by the competition between three main transformations: isomerization, decarboxylation and the addition of water to double bonds. The rates of the three reactions follow the order: isomerization > decarboxylation > hydration. From the result of our HPLC analysis, we identified the presence of MAA, itaconic acid

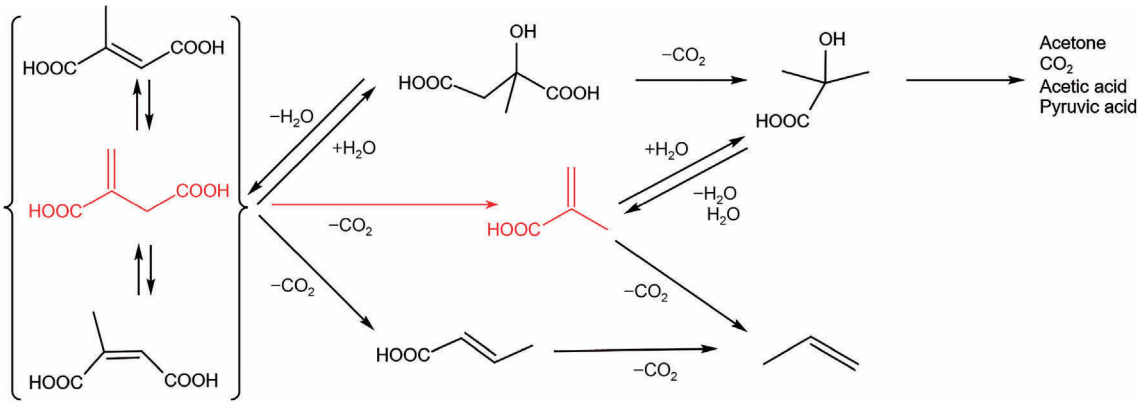

Fig. 3. A possible reaction pathway to itaconic acid decarboxylation to MAA catalyzed by hydroxyapatite.

and its isomers. The crotonic acid and 2-hydroxyisobutyric acid (2-HIBA) were observed in small quantities (<2%). 2-HIBA is unstable and can be degraded under the reaction conditions to pyruvate, acetone and other small molecule gas phase products [21]. Based on the results of our analysis and studies of Li *et al.* and Carlsson *et al.* [20,36], a reaction network was established and is shown in Fig. 3. Itaconic acid firstly isomerized to mesaconic acid and citraconic acid mainly over the weak acid sites of hydroxyapatite. In the second step, abstraction of proton from itaconic acid occurred on the surface of the hydroxyapatite catalyst. The monoanion form of itaconic acid continued to decarboxylation to MAA. Under the reaction conditions, a small amount of MAA and crotonic acid continue to decarboxylate to propylene. Due to the presence of hydroxyapatite acidic sites, the decarboxylation of itaconic acid to MAA is accompanied by the hydration reaction between MAA and itaconic acid isomers to form 2-HIBA and eventual degradation to small molecule products such as acetone. The side-reactions in the system seem to happen at the beginning of reaction.

4. Conclusions

A series of hydroxyapatite catalysts with different Ca/P ratios were prepared, their physical structures and acid-base were characterized, and their catalytic performance for decarboxylation of itaconic acid was evaluated. The results showed that 61.2% yield of MAA was achieved with basically complete conversion of itaconic acid using the hydroxyapatite with a Ca/P of 1.58 in the aqueous phase under the reaction conditions of 1 equivalent of NaOH, 2 MPa of N_2, 250 °C, and 2 h. The efficient conversion of itaconic acid to MAA without the use of precious metals and under milder conditions was achieved, and a reaction network of itaconic acid decarboxylation catalyzed by hydroxyapatite was established. Selective orientation of hydroxyapatite crystals is influenced by the pH of the precursor solution. At a low pH, the preferred orientation of hydroxyapatite crystals is {0 0 2} plane, and the phosphate-bearing faces are largely exposed, resulting in a relatively high density of acid sites. The preferred orientation of hydroxyapatite crystals gradually shifts to {2 1 1} plane by increasing the pH of solution, and the calcium-bearing faces are more highly exposed, resulting in the high basic site density. Only a suitable acidity or alkalinity can provide higher catalytic performance for the decarboxylation of itaconic acid, and the crystal preferred orientation of hydroxyapatite with Ca/P ratio of 1.58 is more conducive to the formation of MAA. The high specific surface area and tunable surface acid-base properties are the main reasons for the high catalytic performance of hydroxyapatite in the decarboxylation of itaconic acid to MAA.

Declaration of Competing Interest

The authors declare that they have no known competing financial interests or personal relationships that could have appeared to influence the work reported in this paper.

Acknowledgements

This work was supported by the National Natural Science Foundation of China (Grant No. 21978066), Basic Research Program of Hebei Province for Natural Science Foundation and Key Basic Research Project (Grant No. 18964308D), and the Key Program of Natural Science Foundation of Hebei Province (Grant No. B2020202048).

Supplementary Material

Supplementary data to this article can be found online at https://doi.org/10.1016/j.cjche.2022.01.012.

References

[1] J. Verduyckt, D.E. de Vos, Controlled defunctionalisation of biobased organic acids, *Chem. Commun. (Camb)* 53 (42) (2017) 5682–5693.
[2] C.Y. Zhou, X.M. Cui, M.H. Li, J.W. Guan, Analysis of market of methyl methacrylate market, *Chem. Ind.* 38 (04) (2020) 80–86.
[3] Y.N. Xu, Production and application of methyl methacrylate, *Refin. Chem. Ind.* 25 (5) (2014) 1–2.
[4] K. Nagai, New developments in the production of methyl methacrylate, *Appl. Catal. A Gen.* 221 (1–2) (2001) 367–377.
[5] Y.H. Hu, G.C. Jiang, G.Q. Xu, X.D. Mu, Hydrogenolysis of lignin model compounds into aromatics with bimetallic Ru-Ni supported onto nitrogen-doped activated carbon catalyst, *Mol. Catal.* 445 (2018) 316–326.
[6] M.J. Darabi Mahboub, J.L. Dubois, F. Cavani, M. Rostamizadeh, G.S. Patience, Catalysis for the synthesis of methacrylic acid and methyl methacrylate, *Chem. Soc. Rev.* 47 (20) (2018) 7703–7738.
[7] P. Gallezot, Conversion of biomass to selected chemical products, *Chem. Soc. Rev.* 41 (4) (2012) 1538–1558.
[8] R. Pirri, J.L. Dubois, Impact Additives, United States Pat., 20120046416 (2012).
[9] J.L. Dubois, Method for Manufacturing a Biomass-Derived Methyl Methacrylate, United States Pat., 20110287991 (2011).
[10] J.L. Dubois, J.F. Crolzy, L. Campora, C. Croizy, P. Croizy, Biomass-derived Methyl Methacrylate and Corresponding Manufacturing Method, Uses and Polymers, United States Pat., 20110318515 (2011).
[11] J.L. Dubois, Method for Manufacturing Biomass-derived Methyl Methacrylate, United States Pat., 20110301316 (2011).
[12] D.W. Johnson, G.R. Eastham, M. Poliakoff, T.A. Huddle, A Process for the Production of (Meth)acrylic Acid and Derivatives and Polymers Produced Therefrom, United States Pat., 20150307433 (2015).
[13] L.L. Zhou, L. Wang, Y.L. Cao, Y.Y. Diao, R.Y. Yan, S.J. Zhang, The states and effects of copper in Keggin-type heteropolyoxometalate catalysts on oxidation of methacrolein to methacrylic acid, *Mol. Catal.* 438 (2017) 47–54.
[14] L.L. Zhou, L. Wang, Y.Y. Diao, R.Y. Yan, S.J. Zhang, Cesium salts supported heteropoly acid for oxidation of methacrolein to methacrylic acid, *Mol. Catal.* 433 (2017) 153–161.
[15] J.L. Ramos, Z. Udaondo, B. Fernández, C. Molina, A. Daddaoua, A. Segura, E. Duque, First- and second-generation biochemicals from sugars: biosynthesis of itaconic acid, *Microb. Biotechnol.* 9 (1) (2016) 8–10.
[16] S.T. Ahmed, N.G.H. Leferink, N.S. Scrutton, Chemo-enzymatic routes towards the synthesis of bio-based monomers and polymers, *Mol. Catal.* 467 (2019) 95–110.
[17] D.W. Johnson, G.R. Eastham, M. Poliakoff, T.A. Huddle. Method of Producing Arcylic and Methacrylic Acid, United States Pat., 8933179 (2015).
[18] D.W. Johnson, G.R. Eastham, M. Poliakoff, T.A. Huddle, Process for the Production of Methacrylic Acid and Derivatives and Polymers Produced Therefrom, United States Pat., 9890103 (2013).
[19] D.W Johnson, G.R. Eastham, M. Poliakoff, T.A. Huddle, A Process for the Production of Methacrylic Acid and Derivatives and Polymers Produced therefrom, Canada Pat., 2825258 (2019).
[20] M. Carlsson, C. Habenicht, L.C. Kam, M.J. Antal, N.Y. Bian, R.J. Cunningham, M. Jones, Study of the sequential conversion of citric to itaconic to methacrylic acid in near-critical and supercritical water, *Ind. Eng. Chem. Res.* 33 (8) (1994) 1989–1996.
[21] J. le Nôtre, S.C. Witte-van Dijk, J. van Haveren, E.L. Scott, J.P. Sanders, Synthesis of bio-based methacrylic acid by decarboxylation of itaconic acid and citric acid catalyzed by solid transition-metal catalysts, *ChemSusChem* 7 (9) (2014) 2712–2720.
[22] M. Pirmoradi, J.R. Kastner, Synthesis of methacrylic acid by catalytic decarboxylation and dehydration of carboxylic acids using a solid base and subcritical water, *ACS Sustainable Chem. Eng.* 5 (2) (2017) 1517–1527.
[23] J.C. Lansing, R.E. Murray, B.R. Moser, Biobased methacrylic acid via selective catalytic decarboxylation of itaconic acid, *ACS Sustain. Chem. Eng.* 5 (4) (2017) 3132–3140.
[24] A. Bohre, U. Novak, M. Grilc, B. Likozar, Synthesis of bio-based methacrylic acid from biomass-derived itaconic acid over Barium hexa-aluminate catalyst by selective decarboxylation reaction, *Mol. Catal.* 476 (2019) 110520.
[25] L.G. Ma, Y.R. Sun, D.L. Li, W.L. Lu, Structure and effect of hydroxyapatite support as well as application in catalyst preparation, *J. Chin. Ceram. Soc.* 47 (12) (2019) 1808–1817.
[26] T. Tsuchida, K.B. Jun, T. Yoshioka, S. Sakuma, T. Takeguchi, W. Ueda, Reaction of ethanol over hydroxyapatite affected by Ca/P ratio of catalyst, *J. Catal.* 259 (2) (2008) 183–189.
[27] B. Yan, L.Z. Tao, Y. Liang, B.Q. Xu, Sustainable production of acrylic acid: catalytic performance of hydroxyapatites for gas-phase dehydration of lactic acid, *ACS Catal.* 4 (6) (2014) 1931–1943.
[28] V.C. Ghantani, S.T. Lomate, M.K. Dongare, S.B. Umbarkar, Catalytic dehydration of lactic acid to acrylic acid using calcium hydroxyapatite catalysts, *Green Chem.* 15 (5) (2013) 1211.

[29] G.S. Guo, Y.X. Sun, Z.H. Wang, H.Y. Guo, Preparation of hydroxyapatite nanorods by homogeneous precipitation method under hydrothermal condition, *Mod. Chem. Ind.* 10 (24) (2004) 43–45.
[30] K. Dokko, S. Koizumi, H. Nakano, K. Kanamura, Particle morphology, crystal orientation, and electrochemical reactivity of $LiFePO_4$ synthesized by the hydrothermal method at 443 K, *J. Mater. Chem.* 17 (45) (2007) 4803.
[31] L. Wang, X.M. He, W.T. Sun, J.L. Wang, Y.D. Li, S.S. Fan, Crystal orientation tuning of $LiFePO_4$ nanoplates for high rate lithium battery cathode materials, *Nano Lett.* 12 (11) (2012) 5632–5636.
[32] H. Aoki, Medical Applications of Hydroxyapatite, Ishiyaku EuroAmerica, Inc., Tokyo, 1994.
[33] J.C. Elliott, Structure and chemistry of the apatites and other calcium orthophosphates 94008066 *Stud. Org. Chem.* 18 (1994) 1.
[34] A.K. Lynn, W. Bonfield, A novel method for the simultaneous, titrant-free control of pH and calcium phosphate mass yield, *Acc. Chem. Res.* 38 (3) (2005) 202–207.
[35] A. Bohre, M.A. Ali, M. Ocepek, M. Grilc, J. Zabret, B. Likozar, Copolymerization of biomass-derived carboxylic acids for biobased acrylic emulsions, *Ind. Eng. Chem. Res.* 58 (43) (2019) 19825–19831.
[36] A.P. Burgard, M.J. Burk, R.E. Osterhout, P. Pharkya. Microorganisms for the Production of Methacrylic Acid, United States Pat., 8241877 (2014).
[37] J. Li, T.B. Brill, Spectroscopy of hydrothermal solutions 18: pH-dependent kinetics of itaconic acid reactions in real time, *J. Phys. Chem. A* 105 (48) (2001) 10839–10845.